Estuarine, Coastal and Shelf Science 82 (2009) 452–460

Contents lists available at ScienceDirect

Estuarine, Coastal and Shelf Science

journal homepage: www.elsevier.com/locate/ecss

Modelling ripple development under non-uniform flow and sediment supply-limited conditions in a laboratory flume

William B. Rauen, Binliang Lin, Roger A. Falconer*

Hydro-environmental Research Centre, School of Engineering, Cardiff University, The Parade, Cardiff CF24 3AA, UK

A R T I C L E I N F O

Article history:
Received 17 September 2008
Accepted 15 February 2009
Available online 25 February 2009

Keywords:
bed form
non-uniform flow
sediment supply-limited condition
Doppler sonar
diverging channel

A B S T R A C T

Results are reported herein of an open channel flow laboratory based study of the development of ripples on a fine silica sand bed, and under non-uniform turbulent subcritical flow conditions. The hydraulic model used included a diverging channel, which resulted in a variation of hydraulic and sediment transport parameters along the channel. Sediment supply limitation occurred during experimentation, impacting bed form development. The overall aim of this study was to improve the understanding and modelling capability of the development of bed forms under limited sediment supply and non-uniform flow conditions. In particular, the applicability of an existing empirical model capable of predicting ripple development was tested for the conditions of this study, using measured ripple dimensions. The ripple height and length results were extracted from detailed bed profile records, obtained using an acoustic Doppler probe traversed longitudinally over the sediment bed, at various experimentation time intervals. It was found that the non-uniform flow conditions affected the development rate of the bed forms, while sediment supply limitation impacted their steady state dimensions. The measured steady state ripple dimensions were lower, on average, than the corresponding equilibrium dimensions predicted using existing empirical equations. Non-uniform flow also caused the simultaneous occurrence of bed forms at different stages of development along the hydraulic model, where 3D and 2D ripples and incipient bed forms were recorded. Such a scenario can occur in estuarine and coastal flows, due to changing hydraulic conditions and/or a limitation of sediment supply. The ripple development model tested was verified for the conditions of this study, with its accuracy being shown to depend on an accurate determination of steady state parameters.

1. Introduction

Bed form development can typically influence the variation of key flow parameters, such as the bed roughness, water levels and the turbulence structure. Bed forms can generate drag due to the pattern of dynamic pressure distribution over their surface (Soulsby, 1997). This causes local accelerations and decelerations of the flow, with energy-consuming lee vortices typically occurring in the troughs of the bed forms (Raudkivi, 1997). Knowledge of such phenomena, and of their effects on the flow characteristics, can greatly benefit the design of rivers and canals, estuarine and coastal modelling studies, flood studies, the estimation of the depth of erosion around structures and rates of sediment transport, etc. The quantification of the bed form development rate, and the corresponding dimensions, can also allow for a better representation of the sediment–water interface in numerical model studies of phenomena such as those described above (Li et al., 2006).

The occurrence of different types of bed forms, such as ripples, dunes or antidunes, on a bed of uniform sediment can be generally predicted using a diagram of the bed form stability fields (Baas, 1999). Such predictions are typically based on values of the representative grain size, d, and the flow velocity, U. As a rule of thumb, ripples do not normally occur if 'd' is of the order of 0.8 mm or greater, or if 'U' is greater than about 1 m/s. A key difference between ripples and other types of bed forms is their relatively small dimensions, which make them 'features contained in the constant shear layer of the flow at the bed' (Raudkivi, 1997). The mechanics of ripple formation, the rate of development and the equilibrium dimensions are all generally independent of the flow depth (Yalin, 1977).

In natural flows, in particular those subjected to transient flow conditions, such as tidal flows in estuaries, bed forms rarely reach true equilibrium state, due to constantly changing hydraulic conditions (Nikora and Hicks, 1997). In particular, the development of bed forms occurring under a sediment supply-limited condition

* Corresponding author.
E-mail address: falconerra@cf.ac.uk (R.A. Falconer).

0272-7714/$ – see front matter © 2009 Elsevier Ltd. All rights reserved.
doi:10.1016/j.ecss.2009.02.015

appears to be significantly affected. Few recent studies have investigated this aspect in detail, with typical examples being the studies of Kleinhans et al. (2002) and Bravo-Espinosa et al. (2003) for alluvial flows, and Bastos et al. (2002) for continental shelf flows. The term 'sediment supply-limited condition' is used herein to represent 'a limitation of available, transportable sediment from which the bed forms are moulded' (Kleinhans et al., 2002). Such a condition can typically occur, for instance, in sand–gravel mixtures due to bed armouring and in areas with an exposed bedrock due to depletion of erodible sediment, where a relatively thin layer of sediment may occur over a sandstone bed. It may also occur in some pool–riffle streams or downstream of a hydropower dam due to upstream sediment deposition. What is common about this type of scenario is that the bed form dimensions, rate of growth and geometric arrangement cannot usually be predicted from the local hydraulics and sediment characteristics, but are partly or completely related to the characteristics of the sediment supply from upstream (Kleinhans et al., 2002). The authors could not find published studies where the quantification of ripple development under a sediment supply-limited condition and non-uniform flow was achieved by using generalised methods, such as given by Nikora and Hicks (1997) and Coleman et al. (2005). It follows that this type of predictive formulations of bed form development appears to lack confirmation for a wider range of flow and sediment transport scenarios and, as a result, the prediction of flow parameters typically relies on assumptions about the state of development of the bed forms (Soulsby, 1997). One further challenge is the determination of the time required for the bed forms to achieve a pseudo steady state, under such variable conditions (Coleman et al., 2005).

Results are reported herein of an open channel experimental investigation of the development of ripples on an initially flat bed of fine silica sand, in turbulent subcritical non-uniform flow conditions. The hydraulic model configuration used in this study included a diverging channel, which was used to promote the variation of flow and sediment transport parameters along the flume. Since no sediment feed system was used, and with the amount of sediment that was recirculating in the flume system being very small, the sediment material required for the development of bed forms originated primarily from the eroded bed material in the narrower upstream channel. Depletion of the supply region eventually created a sediment supply-limited condition that would affect the development of the bed form field. These experimental features related the study, with an element of generality, to conditions often found in the field and where ripples, etc form downstream of a non-sedimentary bed, or where the changing hydraulic conditions do not allow for the true equilibrium state to be reached. The main specific aim of the study was to test the applicability of an existing ripple development model, looking to extend its validity for such conditions.

2. Background

The sediment material required for the development of bed forms is provided primarily by the bed load under conditions of excess bed shear stress, i.e. when $\theta \geq \theta_{cr}$, with θ and θ_{cr} being defined as (Soulsby, 1997):

$$\theta = \frac{\tau_b}{(\rho_s - \rho)gd} = \frac{u_*^2}{gd\Delta} \tag{1}$$

$$\theta_{cr} = \frac{0.30}{(1 + 1.2D_*)} + 0.055\left[1 - e^{(-0.02D_*)}\right] \tag{2}$$

where $D_* = d(g\Delta/\nu^2)^{1/3}$ is the dimensionless grain size, d is the representative grain size (taken as the median particle diameter herein), τ_b is the bed shear stress, g is gravitational acceleration, ρ_s and ρ are the densities of the sediment and fluid respectively, and $\Delta = (\rho_s - \rho)/\rho$.

The most commonly used parameters to describe ripple height and length, i.e. η and λ respectively, are the median and/or the maximum values, as reported by several authors. Without resorting to complex morphodynamic numerical models, modelling the current-induced development of ripples on a sediment bed can, at present, be achieved through the use of general empirical formulations for η and λ, such as proposed by Nikora and Hicks (1997) and Coleman et al. (2005). In using such methods, the evolution of the ripple height and length is presumed to follow an empirically observed trend, being a function of their steady state counterparts and the time for the steady state to be reached. The ripple development model of Coleman et al. (2005) appears to incorporate the most recent advancements in this area, predicting the evolution of ripple dimensions to occur according to a power law, as:

$$\eta = \eta_{ss}\left(\frac{t}{t_{ss}}\right)^{0.22D_*^{0.22}} \tag{3}$$

$$\lambda = \lambda_{ss}\left(\frac{t}{t_{ss}}\right)^{0.14D_*^{0.33}} \tag{4}$$

where t is the time and the subscript 'ss' refers to the steady state.

Provided that sediment supply is enough, ripples tend to eventually reach the equilibrium stage, in the sense described by Raudkivi (1997) and others, and their dimensions can be estimated using empirical formulae (Yalin, 1985; Baas, 1993; Raudkivi, 1997; Soulsby and Whitehouse, 2005). The value of t_{ss} associated with such equilibrium stage can typically range from several minutes to hundreds of hours, depending on the excess shear stress condition (Baas, 1994; Raudkivi, 1997; Coleman et al., 2005). Equations (3) and (4) are reportedly valid in the interval of $0.01 < t/t_{ss} < 1.0$, which excludes the steady state stage and, typically, the very early period of formation, when the bed forms are in an incipient stage (Baas, 1994; Coleman and Melville, 1996).

However, substantial errors can occur in predictions made using the above practice when the flow and sediment transport conditions deviate from the case of uniform flow with unlimited supply. This is because the rate of bed form development is primarily governed by the bed load transport rate (Soulsby, 1997), being also affected by the grain size and flow conditions (Coleman and Melville, 1994). It follows that bed form development can be delayed or accelerated under non-uniform flow with a variable sediment supply, while the equilibrium stage may not be reached at all, in particular, when the sediment supply becomes critically limited (Kleinhans et al., 2002). In such a scenario, the steady state ripple dimensions can be much lower than the equilibrium stage estimates, while their geometric nature might be incompliant with the typically observed 3D equilibrium ripples. It is noteworthy that a 2D ripple is generally defined as having the length of its crest considerably larger than the height (Soulsby and Whitehouse, 2005).

A scenario involving the occurrence of a suite of bed form types in an overall framework of limited sediment supply was reported, for instance, by Bastos et al. (2002). In their study, the presence of an area of exposed bedrock on the seabed impacted the supply of sediment material to the further development of bed forms in the nearby region. In alluvial and laboratory flows, Kleinhans et al. (2002) also reported the simultaneous occurrence of different types of bed forms under a sediment supply-limited condition, which occurred as a result of bed armouring that took place due to a nonhomogeneous bed sediment composition. It follows that having a good knowledge of the site characteristics and hydrodynamics is key for achieving a better understanding of the pattern of development of bed forms, especially when occurring under limited sediment supply conditions. It is unclear whether the pattern of ripple development occurring under such conditions follows the trends of Equations (3) and (4). Presuming the general validity of such a model, different constraints may need to be applied to improve confidence in any predictions thus made. The first aspect can be investigated by comparing the model predictions with recorded time series of ripple development obtained under supply-limited conditions and non-uniform flow, with the values of η_{ss}, λ_{ss} and t_{ss} being extracted from such a record, rather than estimated using existing equations for the equilibrium stage. Further analysis of the observed bed forms could help to identify any new constraints required for model application. These aspects were studied herein using experimental data obtained as described in the following section.

3. Experimental work

3.1. Hydraulic model

The hydraulic model used in this study was formed by three main regions, namely a 3.0 m long upstream channel, a 6.0 m long diverging channel and a 4.0 m long downstream channel, as illustrated in Fig. 1. In terms of flume coordinates, the upstream channel occupied the region of $2.0\ \text{m} < x < 5.0\ \text{m}$ and the diverging channel was located between $5.0\ \text{m} < x < 11.0\ \text{m}$, while the downstream channel occupied the region of $11.0\ \text{m} < x < 15.0\ \text{m}$. The width of the upstream and downstream channels was 0.3 m and 0.9 m respectively, while that of the diverging channel increased linearly in the streamwise direction, from 0.3 m to 0.9 m, with a 1:10 aspect ratio. Such a threefold increase in the flow width along the diverging channel allowed for a decrease of hydraulic parameters, causing non-uniform flow.

The hydraulic model was built inside a large flume located in the Hyder Hydraulics Laboratory, at Cardiff University. The amount of sediment recirculating in the flume system was very small and no sediment feed system was used in the experiments. Sediment supply for the development of bed forms along the hydraulic model originated primarily from net erosion of the upstream channel bed, as explained below. Further details about the hydraulic system can be found in Rauen et al. (2008a).

3.2. Sediment characteristics and threshold of motion

Fine quartz sand was used to fill the bed of the hydraulic model, up to the initial bed level of 0.1 m. Key grain size characteristics of the sand were $d = d_{50} = 130\ \mu\text{m}$, $d_g = 120\ \mu\text{m}$ and $\sigma_g = 2$, where d_{50} is the median grain size, $d_g = (d_{84}d_{16})^{0.5}$ is the geometric mean grain size and $\sigma_g = (d_{84}/d_{16})^{0.5}$ is the geometric standard deviation of sediment sizes. The relatively low value of σ_g indicated that the sand was well sorted and relatively uniform. The settling velocity, dimensionless grain size, critical Shields parameter and critical friction velocity were calculated using standard formulations (Soulsby, 1997), as $w_s = 1.2$ cm/s, $D_* = 3.3$, $\theta_{cr} = 0.065$ and $u_{*cr} = 1.2$ cm/s respectively. Pebbles with $d \approx 1$ cm were introduced at the inlet section of the model, prior to the upstream channel, i.e. in the region of $0.0\ \text{m} < x < 3.0\ \text{m}$, as a replacement for the sand. This was done to raise the sediment bed height with a mild slope, while preventing erosion of the inlet region. The interface between the pebbles and sand occurred at $x = 3.0$ m, i.e. inside the upstream channel. Only the sandy part of the hydraulic model, comprising the region of $3.0\ \text{m} < x < 15.0\ \text{m}$, was investigated for the development of bed forms, since the experimentation conditions did not allow for movement of the pebbles.

3.3. Experimental conditions

The sediment bed was flattened prior to the start of an experiment. Freshwater was then introduced in the flume via two side channels and the hydraulic model was filled slowly, so as not to disturb the flattened sediment bed. The experimental water depth was 0.4 m above the flume bed, which gave a depth of $H = 0.3$ m above the initial bed level. By taking into account this water depth in the model, the critical mean streamwise velocity for sediment erosion in the flat bed condition was estimated as being $U_{0cr} \approx 25$ cm/s. This value was obtained using a power law fit for steady currents on flat beds, which reads (Soulsby, 1997):

$$U_{0cr} = 7u_{*cr}\left(\frac{d}{H}\right)^{-\frac{1}{7}} \tag{5}$$

The flow rate used in the hydraulic model experiments was $Q = 45$ l/s. This value resulted in a turbulent and subcritical flow, as indicated by the bulk Reynolds and Froude numbers, calculated as $\text{Re} = U_0 4R_h/\nu$ and $\text{Fr} = U_0/(gH)^{0.5}$ respectively, where R_h is the hydraulic radius. The cross-sectional mean streamwise velocity in the upstream channel was estimated as $U_0 = 50$ cm/s, where $U_0 = Q/A$ and A is the cross-sectional area of the flow. The ranges calculated for these parameters were $170{,}000 < \text{Re} < 115{,}000$, $0.3 < \text{Fr} < 0.1$ and $50\ \text{cm/s} < U_0 < 17\ \text{cm/s}$, with the higher values occurring in the upstream channel. The flat bed distribution of the relative Shields number, i.e. θ/θ_{cr}, was used as an indication of the likelihood of net erosion in different parts of the model, where θ and θ_{cr} were calculated using Equations (1) and (2) respectively. Erosion of the flat sand bed was not expected to occur for $x > 8.0$ m approximately, since $\theta/\theta_{cr} < 1$ for that region. The maximum rate of erosion expected was for the upstream channel, with $\theta/\theta_{cr} \approx 4.0$. The particle Reynolds and Froude numbers were calculated as $\text{Re}_* = u_*d/\nu$ and $\text{Fr}_* = U_0/[gd(s-1)]^{0.5}$ respectively and the corresponding ranges were $3.0 < \text{Re}_* < 1.0$ and $10.0 < \text{Fr}_* < 4.0$, indicating a hydrodynamically smooth flow. Such a flow condition was conducive to the formation of ripples (Raudkivi, 1997; Karim, 1999). The parameter u_*/w_s was always lower than 2.0 in the hydraulic model experiments. Four experiments were conducted under similar conditions, as described above, with the bed profile being frequently measured to assess bed form development.

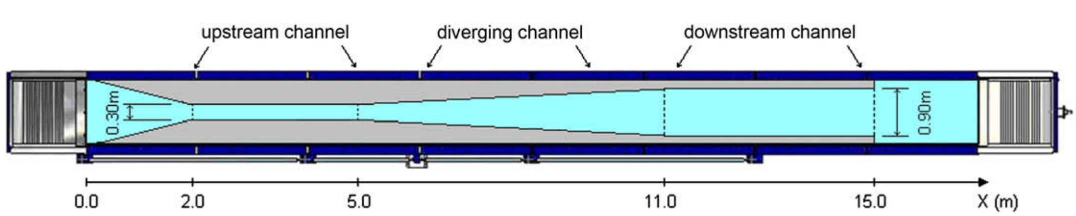

Fig. 1. Schematic diagram of the hydraulic model inside the experimentation flume, highlighting the location of the upstream, diverging and downstream channel reaches and key dimensions. The flow in a typical experiment was from left to right.

3.4. Bed form data acquisition and processing

The bed profile measurements were carried out using an Acoustic Doppler probe, i.e. Nortek's Vectrino^{+}, operated in sonar mode and automatically traversed along the x direction centreline of the flume. The longitudinal positions and bed elevation values thus obtained were combined to generate 2D profiles of the bed. The accuracy of the method, when used under the experimentation conditions reported herein, was similar to that of a commercial bed profiler equipped with a conductivity probe. Fig. 2 illustrates a comparison of typical results obtained for a reach of rippled bed, where the corresponding bed profile records were practically coincident. The accuracy of the commercial bed profiler has been prescribed as being of order of 1 mm in the vertical direction. The spacing in the longitudinal direction between data points was around 6 mm. With regard to assessments of the ripple dimensions, Raudkivi (1997) pointed out that the measurement of single longitudinal bed profiles can only yield meaningful results when the rippled bed is more or less 2D, since for a 3D ripple pattern a significant amount of the measured 'peaks' would lie on the flanks of the ripples. This would lead to a lower than true mean ripple height being calculated for such a region, and was taken into consideration during the data analysis (as further discussed below).

Bed profile measurements in this study were carried out at various experimentation time intervals, from $t = 0.5$ h to $t = 24$ h. For carrying out such measurements the pump was slowly ramped down to reduce the flow rate, so that the bed shear stresses anywhere in the model were significantly below the threshold of motion. Each bed profile assessment lasted typically between 20 and 30 min, after which time the pump was slowly ramped up to the experimental flow rate, and the experiment continued. The experimentation time intervals referred to herein was computed by discounting the periods when the pump was operating at any flow rate value other than the experimental flow rate. The processing of bed profiling data involved searching the records for bed surface slopes, so that the slope inflection points in a bed profile could be identified. The height difference between a trough and the subsequent crest in the upstream direction was calculated. Height values above $10d$ were marked and recorded, together with the corresponding position along the x direction. Median height and length values, represented by η_{50} and λ_{50} respectively, were calculated at a 1.0 m step along the longitudinal direction of the model. The results thus obtained were then associated with the central point of the corresponding intervals. For instance, station $x = 7.0$ m represented the median data calculated between $6.5\ \text{m} < x < 7.5\ \text{m}$, while the data measured in the region of $7.0\ \text{m} < x < 8.0\ \text{m}$ was used to compute the results associated with station $x = 7.5$ m, etc.

4. Results and discussion

This section starts with an analysis of the effects of non-uniform flow and sediment supply limitation on the pattern of bed form development occurring in the hydraulic model experiments, using photographic evidence and measured time series of ripple dimensions. The steady state ripple height, length and time, i.e. η_{ss}, λ_{ss} and t_{ss} respectively are then determined based on calculated results for the growth rate of the bed forms. Finally, the ripple development model is verified against experimental data.

4.1. Overview of bed form development – effects of non-uniform flow

The centreline bed profiles measured in one of four experiments conducted are shown in Fig. 3, for the assessment times in the interval of $0.5\ \text{h} < t < 24$ h. These records encompassed the region of $4.0\ \text{m} < x < 12.0$ m, which included a 1.0 m reach of the upstream channel, the full length of the diverging channel and a 1.0 m reach of the downstream channel (see Fig. 1). The plotted results have been filtered to remove the macro-scale bed level changes that took place in the experiment due to net erosion or deposition, allowing for a better representation of the smaller scale bed forms. These transects were then used to calculate the distribution of the median bed form height and length, i.e. η_{50} and λ_{50} respectively along the hydraulic model, as further discussed below.

Key stages of bed form development observed in different regions of the hydraulic model are illustrated in Fig. 4, where the flow direction was from left to right. Fig. 4a depicts the rippled field observed at $t = 1.0$ h in the region comprising the end of the upstream channel and the initial part of the diverging channel. The occurrence of 3D and 2D ripples in this region can be noted at this time, with a zone of transition from 3D to 2D ripples occurring inside the diverging channel. At $t = 24$ h, such a transition zone was typically located near $x \approx 7.5$ m. In most of the diverging channel reach, the ripple field retained a 2D character until the end of experimentation, as shown in Fig. 4b, for the region near $x = 9.0$ m. Fig. 4c illustrates the development of bed forms in the area around the interface between the diverging and downstream channels, i.e.

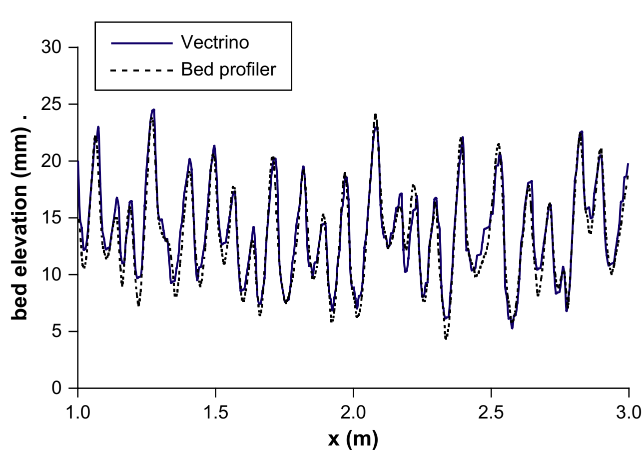

Fig. 2. Comparison between bed profile measured with a conventional bed profiler, equipped with a conductivity probe, and the corresponding record obtained with the Vectrino^{+}.

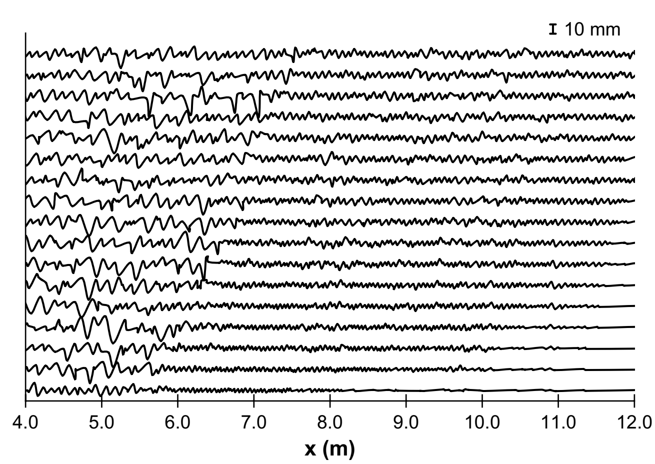

Fig. 3. Centreline transects measured in the hydraulic model experiments in the following experimentation time intervals: $t = 0.5$, 1.0, 1.5, 2.0, 2.5, 3.0, 3.5, 4.0, 5.0, 6.0, 7.0, 8.0, 11, 14, 17, 20 and 24 h. The region showing a higher bed form amplitude, on the left hand side of each record, denoted the occurrence of 3D bed forms.

near $x = 11.0$ m, for the experimentation time intervals of $t = 3.0$, 4.5, 6.0 and 9.0 h. These photographs confirmed that bed form development occurred in this region, despite the relatively low values of the bed shear stresses encountered there – with $\theta/\theta_{cr} < 1.0$ being estimated for flat bed condition. A comparison of subsequent images in Fig. 4c suggested that bed form development in this region was induced by an increase in the bed roughness that took place as a result of development of the upstream ripple field, in accordance with the observations of Baas and Best (2000). Fig. 4c further suggests that the rate of bed form development was higher near the channel centreline than near the walls. Such a non-uniform pattern of bed form development across the channel was probably caused by non-uniform flow in the lateral direction. Visual observations suggested that the bed forms in the latter zone did not develop further than the incipient stage, in the sense described by Baas (1994), even at later experimentation time intervals. Overall, the photographic analysis indicated that non-uniform flow induced the occurrence of distinct patterns of development for the bed forms in the hydraulic model. In particular, a pattern of decreasing development rates occurred due to the decreasing hydro-sedimentological conditions along the streamwise direction – a diverging channel effect. This observation is discussed further below, based on the measured ripple dimensions.

Fig. 5 illustrates the time series variation of the median bed form dimensions obtained in four hydraulic model experiments, with Fig. 5a–c including the results for the regions centred at $x = 3.5$ m, 8.0 m and 11.5 m respectively. These plots illustrate the different patterns of bed form development observed in distinct regions of the hydraulic model. For instance, in the region of $x = 3.5$ m (Fig. 5a) the data showed a high level of scatter, in particular in the interval of $t < 8.0$ h, probably due to the 3D nature of the bed form field in this region. No clear trend could be identified in these results, besides the fact that the η_{50} and λ_{50} values appeared to become asymptotic after a while. The highest excess bed shear stresses found in the hydraulic model experiments occurred in this region, with $\theta/\theta_{cr} \approx 4.0$ being estimated for the flat bed condition. This induced a relatively high rate of bed form development, with the ripples quickly assuming a 3D character, as illustrated in Fig. 4a. On the other hand, in the region of $x = 8.0$ m (Fig. 5b), where the bed shear stresses were around the threshold of motion, the ripple dimensions increased monotonically from the start of monitoring, before also tending to an asymptote. As shown in Fig. 4b, the bed forms in this region retained a 2D character during the experiment. Finally, in the region of $x = 11.5$ m (Fig. 5c), where the bed shear stresses were relatively low, the bed form dimensions were approximately constant in the time interval of $0.0 < t < 3.0$ h. This

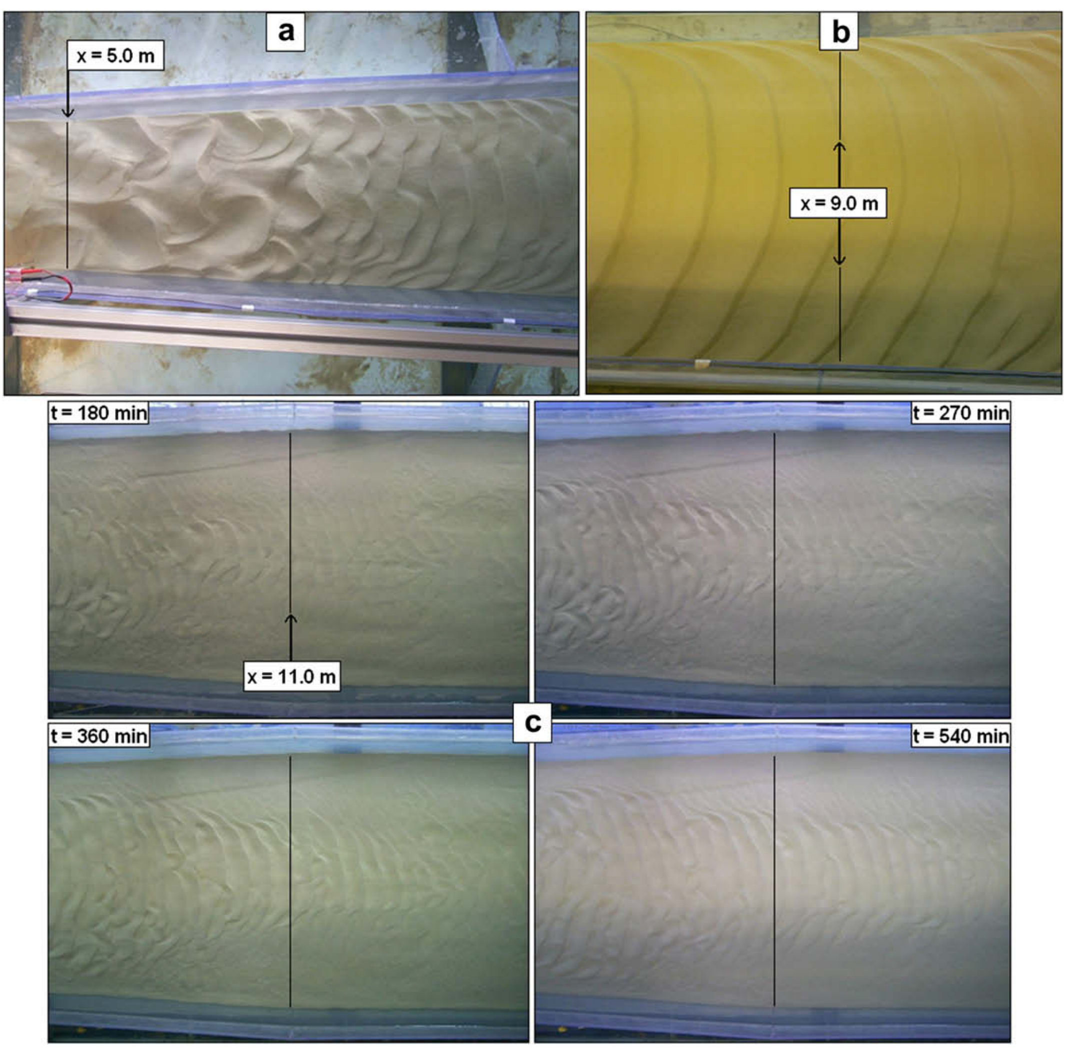

Fig. 4. Photographic illustration of bed form development along the hydraulic model, showing the regions located at: (a) end of upstream channel and start of diverging channel at $t = 1.0$ h; (b) diverging channel at $t = 24$ h; (c) time variation of ripple bed at interface between diverging and downstream channels.

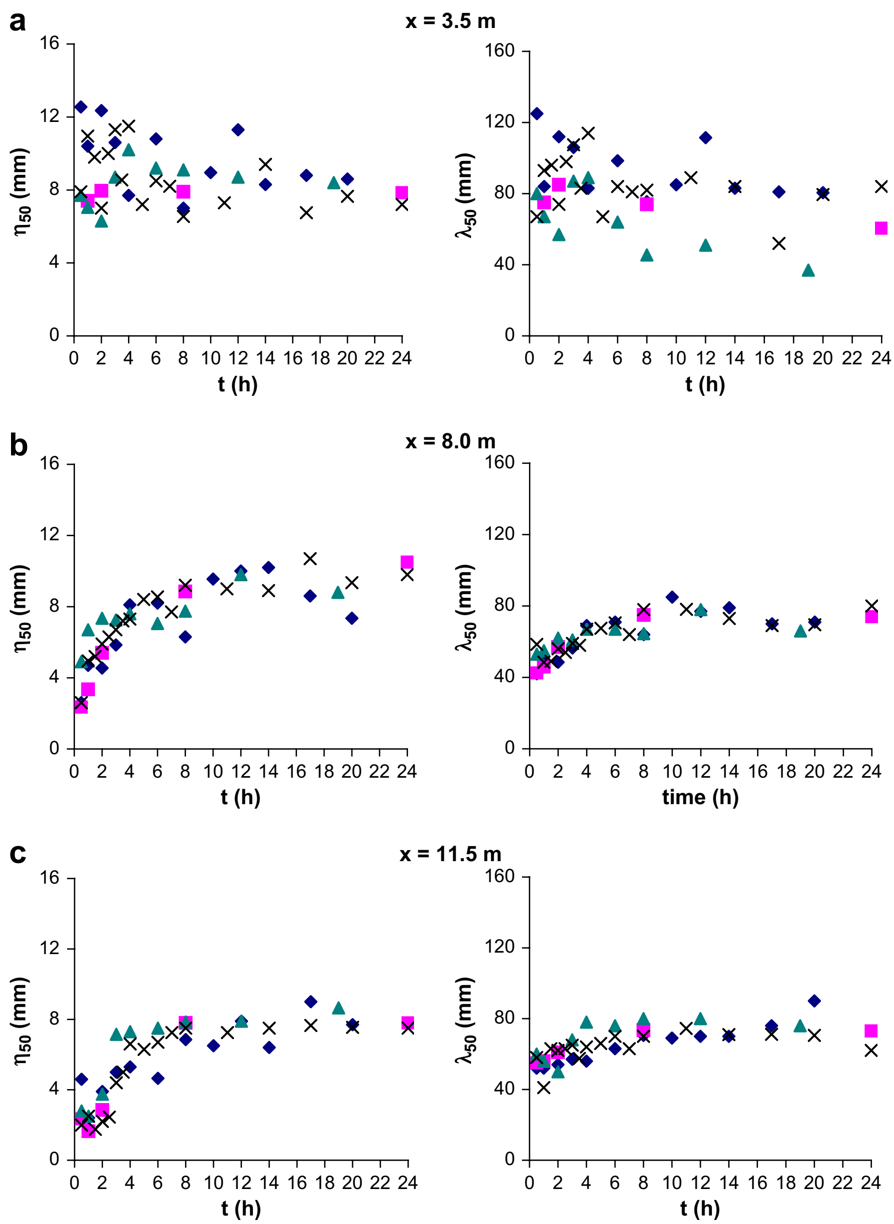

Fig. 5. Variation in time of the median bed form height (η_{50}) and length (λ_{50}) in the regions of: (a) $x = 3.5$ m; (b) $x = 8.0$ m; (c) $x = 11.5$ m. The different markers indicate results from four independent experiments conducted under similar conditions.

was followed by a period of increase of η_{50} and λ_{50}, prior to these parameters tending to an asymptote also at this site. These results can be related to the comments previously made on Fig. 4c, where the development of bed forms was probably eventually induced by an increase of the upstream bed roughness. The simultaneous occurrence of a suite of bed form types, as reported herein for the hydraulic model experiments, is not, in itself, an unusual phenomenon. However, such a condition appears to be normally associated with a heterogeneous sediment distribution (Bastos et al., 2002; Kleinhans et al., 2002). On the other hand, in the present study the bed was homogeneous in terms of sediment particle sizes. It follows that the photographic assessment and the measured bed form dimensions both confirmed that the occurrence of non-uniform flow along the hydraulic model induced different patterns of bed form development, with the rate of development being the key parameter affected.

4.2. Determination of the steady state – effect of sediment supply limitation

In this study, the steady state was deemed to occur when the bed form dimensions tended to an asymptote, in terms of the trends of the η_{50} and λ_{50} results. In order to determine this, the measured results were used to calculate the development rate of the bed forms. These calculations were made for the zone of 2D ripples that occurred in the diverging channel, i.e. the region of $7.5\ \mathrm{m} < x < 11.0\ \mathrm{m}$, in order to minimise errors due to the occurrence of 3D and incipient bed forms. The development rate was calculated as:

$$\frac{\mathrm{d}\varphi_{50}}{\mathrm{d}t} = \left|\frac{\varphi_{50_i} - \varphi_{50_{i-1}}}{t_i - t_{i-1}}\right| \tag{6}$$

where φ represented generally a bed form dimension and 'i' represented an assessment time in the interval of $0.5\ \mathrm{h} < t < 24\ \mathrm{h}$. The results obtained for the average development rate of η_{50} and λ_{50} in the region of 2D ripples in the hydraulic model are plotted in Fig. 6a and b respectively, as a function of the upper limit of the corresponding time intervals. It can be seen that the development rate was relatively high in the early stages of experimentation and, in particular, for $t = 1.0$ h, when a typical rate was around 3.0 mm/h for η_{50} and 14 mm/h for λ_{50}. Subsequently, the development rates decreased according to a power law, before tending to an asymptote. The asymptotic levels observed for η_{50} and λ_{50} were around 0.3 mm/h and 1.6 mm/h respectively, which were smaller than the resolution of measurements (as outlined above) and regarded as random variations due to phenomena such as migration, coalescence, etc. The time for the steady state was estimated from the results shown in Fig. 6, as being $t_{ss} = 11$ h for the bed form height results, and $t_{ss} = 14$ h for the bed form length, which were relatively low, considering the excess shear stress condition ($\theta/\theta_{cr} \approx 1$) (Raudkivi, 1997; Coleman et al., 2005). This was caused by sediment supply becoming critically limited during the experiments, as suggested by the fact that the bed form dimensions entered a steady state as the net erosion rate of the upstream channel bed tended to zero (Rauen et al., 2008b). While t_{ss} and other steady state parameters can be sensitive to the variation of the sediment supply levels, this study was primarily concerned with verifying the ripple development model under such experimental conditions, as further discussed in a following section.

The steady state bed form dimensions were calculated as the average η_{50} and λ_{50} results occurring in the interval of $t_{ss} < t < 24$ h along the hydraulic model, as shown in Fig. 7. It can be noted from these results that the values of η_{ss} and λ_{ss} generally decreased with x due to non-uniform flow conditions, indicating that the bed forms along the assessment region were in distinct stages of development when the steady state was reached. The trends of η_{ss} and λ_{ss} were similar, while the ratio between these parameters was calculated as $\lambda_{ss}/\eta_{ss} = 8.60$, on average. This value was close to the inverse of the steepness value predicted for the sand of this study of 8.06 (Raudkivi, 1997; Rauen et al., 2008a).

The ranges obtained for the steady state bed form dimensions were 8.4 mm $< \eta_{ss} <$ 10.5 mm and 71 mm $< \lambda_{ss} <$ 93 mm. It can be noted that the asymptotic ripple dimensions obtained experimentally by Mantz (1978, 1983, 1992) for a comparable type of sediment with $d = 0.12$ mm lie within these ranges (Mantz experimental values: $\eta_{ss} = 8.7$ mm and $\lambda_{ss} = 81$ mm). On the other hand, using predictive equations of equilibrium ripple dimensions (Yalin, 1985; Baas, 1993; Raudkivi, 1997; Soulsby and Whitehouse, 2005) would yield values in the ranges of 10–15 mm for η, and 113–131 mm for λ. These values are around 30% higher, on average, than the η_{ss} and λ_{ss} obtained experimentally herein and by Mantz. What such a discrepancy suggests is that the bed forms did not reach the equilibrium stage, in the sense described by Baas (1993) and Coleman and Melville (1994), although the ripple height and length entered a steady state. This can be an effect of sediment supply limitation, as shown by Kleinhans et al. (2002). It is noteworthy the fact that the experimental apparatus used in Mantz's experiments (described by Mantz, 1980) has two key similarities with the experiments for the present paper: (1) a sediment feed system is not used; (2) the amount of sediment recirculating in the system water is negligible. These features combined can typically lead to degradation of the mobile sediment bed, due to sediment transport occurring at below capacity conditions. This scenario occurred in the hydraulic model experiments and reportedly occurred in Mantz' experiments (Mantz, 1992). Under such a condition of non-equilibrium sediment transport, the eroding bed acted as the primary source of sediment for the transport processes that developed further downstream in the channel, including bed form development associated with the bed load. It follows that once the erosion depth reached the depth of the sand bed laid for the experiments – or the bed shear stress fell below the critical value for sediment mobilisation due to the enlarged flow depth – then sediment supply became critically limited, halting bed form development. Such a steady state scenario occurred prior to the equilibrium stage being reached, with the asymptotic bed form dimensions being lower than the equilibrium dimensions. In theory, this should not represent an impediment for the application of the model of Coleman et al. (2005) and other similar models of bed form development, although this model may have to be adapted for such conditions – this being the subject of a following section in this paper. It is anticipated that the spatial variation of η_{ss} and λ_{ss} should be taken into account when using such a ripple development model under limited sediment supply conditions.

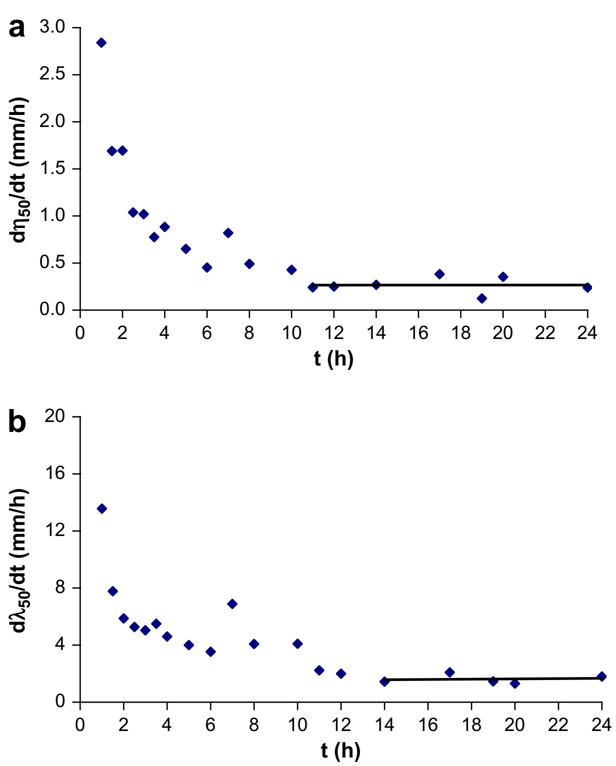

Fig. 6. Variation in time of the development rate of bed forms, showing the results for: (a) bed form height; (b) bed form length. The straight lines shown indicate the asymptotic level.

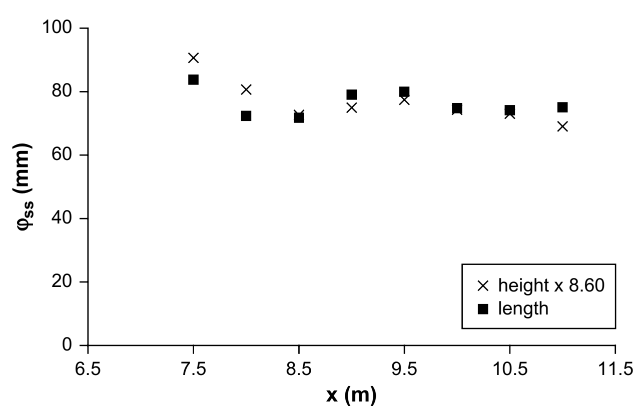

Fig. 7. Variation of the steady state bed form dimensions along the hydraulic model, with the bed form height results multiplied by the calculated ripple steepness of 8.60.

4.3. Verification of the ripple development model of Coleman et al. (2005)

The steady state dimensions and time obtained as discussed above were used as input parameters to Equations (3) and (4), in predicting the variation of bed form dimensions with the time in the hydraulic model. In these calculations, η and λ were taken as the median bed form height and length results, which were normalised by the corresponding steady state dimensions. A comparison of the predictions obtained using the model of Coleman et al. (2005) and the experimental data of this study is shown in Fig. 8a and b, for the bed form height and length results respectively. Overall, the agreement between the data and the corresponding prediction was good, confirming the appropriateness of using the above mentioned ripple development model for the experimental conditions of this study. Considering that the first set of results used herein was for $t = 0.5$ h, the model was applied in the time interval of $0.03 < t/t_{ss} < 1.0$, which is inside the prescribed time range (Coleman et al., 2005). These results further suggested that the conditions of non-uniform flow and limited sediment supply did not affect the model's predictive ability – but it was key to use empirically determined values of the steady state parameters as inputs to the model. Had the model been applied using equilibrium dimensions and time estimated for the sand of this study – which are significantly higher than the measured steady state parameters – then the predictions would show a poor agreement with the data and the model would fail. This fact confirmed the need for a case-specific determination of the steady state quantities when the developing bed forms are subjected to limited sediment supply conditions.

The limitation of the sediment supply levels occurred as the erosion rate in the upstream channel bed tended to zero, which caused bed form development to come to a halt. While the link between sediment supply limitation and bed form development has been demonstrated qualitatively before (e.g. by Kleinhans et al., 2002), this study quantified bed form development under such conditions without having to resort to complex and computationally demanding morphodynamic models. Key to the study was the fact that sediment transport occurred at below capacity conditions, which varied in time and reached a critically limited stage that impacted bed form development significantly. These conditions are not uncommon in estuarine systems, in particular in the vicinity of bedrock (Bastos et al., 2002). In spite of this scenario, the variation of the normalised bed form height and length with the time along a region subjected to spatially varied hydro-sedimentological conditions (i.e. the divergent channel) closely followed the trend currently associated with bed form development occurring under plentiful sediment supply leading to the equilibrium stage, and typically under uniform flow conditions. This can have implications for achieving an improved representation of the sediment–water interface in models of estuarine flows, in particular when determining the bed roughness scale dynamically. By reducing the uncertainty involved in such hydrodynamic models, other related sediment transport and water quality studies made for these regions will also be benefited.

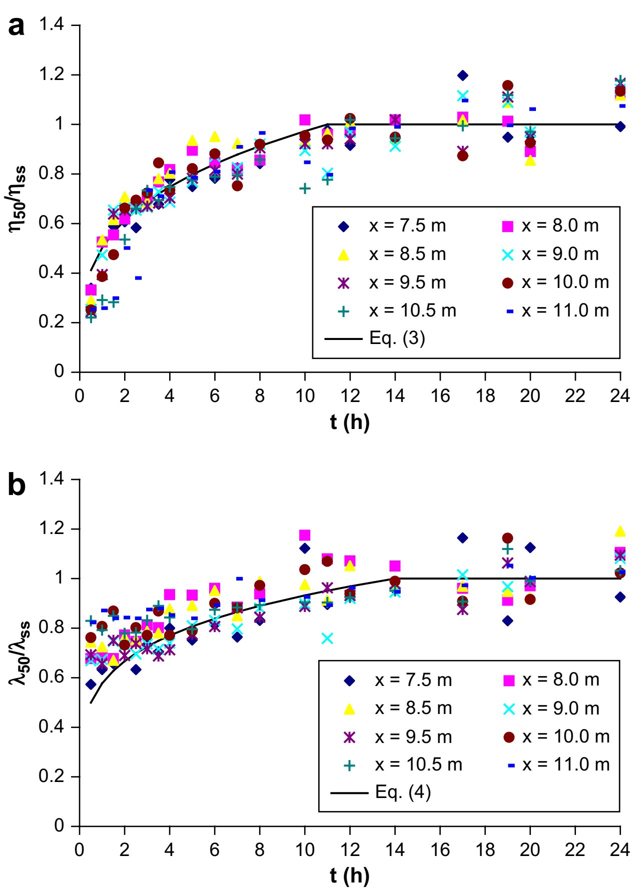

Fig. 8. Variation in time of the normalised bed form dimensions, showing the results for: (a) bed form height; (b) bed form length. The markers indicate experimental results calculated for various sites along the diverging channel, while the curves corresponding to Equations (3) and (4) represent the predictions made with the ripple development model of Coleman et al. (2005).

5. Conclusion

This study was carried out to investigate the development of ripples on a fine silica sand bed of an open channel flow laboratory model. The hydraulic model used included a diverging channel, which resulted in a variation of the hydraulic and sediment transport parameters along the channel. Sediment supply limitation occurred during the experimentation, impacting bed form development. Measurements were made of the bed profile variation in time, with the bed form dimensions being extracted from such records and later used to investigate their pattern of development. An empirical model, developed to predict the variation of the ripple height and length under unlimited sediment supply and uniform flow conditions (see Coleman et al., 2005) was applied under sediment supply-limited conditions and non-uniform flow.

Non-uniform flow conditions in the hydraulic model experiments impacted the development rate of bed forms and induced the simultaneous occurrence of a range of bed form types, which generally included incipient bed forms and 2D and 3D ripples. The bed forms did not reach the equilibrium stage in the experiments, because sediment supply became critically limited during their development. Instead, a steady state was observed in terms of the bed form dimensions and spatial distribution, as often also found in nature. A good agreement was observed between the data and model predictions for the normalised ripple dimensions, as the overall trend of ripple development was not impacted by the limitation of sediment supply and variation of the development rate. However, the successful application of such a model to the conditions of this study was shown to require the use of measured steady state ripple height, length and time, rather than estimated values corresponding to the equilibrium stage. Further studies will focus on verifying the findings reported herein to other sediment sizes and flow conditions.

Acknowledgements

Receipt of the equipment grant NE/C513269/1 from the UK's Natural Environment Research Council (NERC), and the research grant EP/C512316/1 from the Engineering and Physical Sciences Research Council (EPSRC) is greatly acknowledged by the authors. We would also like to thank Mr. Paul Leach for the technical support provided during the experimental work.

References

Baas, J.H., 1993. Dimensional analysis of current ripples in recent and ancient depositional environments. PhD Thesis, University of Utrecht, The Netherlands.
Baas, J.H., 1994. A flume study on the development and equilibrium morphology of current ripples in very fine sand. Sedimentology 41, 185–209.
Baas, J.H., 1999. An empirical model for the development and equilibrium morphology of current ripples in fine sand. Sedimentology 46, 123–138.
Baas, J.H., Best, J.L., 2000. Ripple formation induced by biogenic mounds – comment. Marine Geology 168, 145–151.
Bastos, A.C., Kenyon, N.H., Collins, M., 2002. Sedimentary processes, bedforms and facies, associated with a coastal headland: Portland Bill, Southern UK. Marine Geology 187, 235–258.
Bravo-Espinosa, M., Osterkamp, W.R., Lopes, V.L., 2003. Bedload transport in alluvial channels. Journal of Hydraulic Engineering 129 (10), 783–795.
Coleman, S.E., Melville, B.W., 1994. Bed-form development. Journal of Hydraulic Engineering 120 (4), 544–560.
Coleman, S.E., Melville, B.W., 1996. Initiation of bed forms on a flat sand bed. Journal of Hydraulic Engineering 122 (6), 301–310.
Coleman, S.E., Zhang, M.H., Clunie, T.M., 2005. Sediment–wave development in subcritical water flow. Journal of Hydraulic Engineering 131 (2), 106–111.
Karim, F., 1999. Bed-form geometry in sand-bed flows. Journal of Hydraulic Engineering 125 (12), 1253–1261.
Kleinhans, M.G., Wilbers, A.W.E., de Swaaf, A., van den Berg, J.H., 2002. Sediment supply limited bedforms in sand–gravel bed rivers. Journal of Sedimentary Research 72 (5), 629–640.
Li, M., Pan, S., O'Connor, B.A., 2006. Modelling coastal boundary layer flows over typical bed-forms. Proceedings of the Institution of Civil Engineers, Maritime Engineering 159 (MA1), 9–24.
Mantz, P.A., 1978. Bed forms produced by fine, cohesionless, granular and flakey sediments under subcritical water flows. Sedimentology 25, 1–21.
Mantz, P.A., Dec, 1980. Laboratory flume experiments on the transport of cohesionless silica silts by water streams. Proceedings of the Institution of Civil Engineers, Part 2 69, 977–994.
Mantz, P.A., 1983. Semi-empirical correlations for fine and coarse cohesionless sediment transport. Proceedings of the Institution of Civil Engineers, Part 2 75 Paper 8594.
Mantz, P.A., 1992. Cohesionless, fine sediment bed forms in shallow flows. Journal of Hydraulic Engineering 118 (5), 743–764.
Nikora, V.I., Hicks, D.M., 1997. Scaling relationships for sand–wave development in unidirectional flow. Journal of Hydraulic Engineering 123 (12), 1152–1156.
Raudkivi, A.J., 1997. Ripples on stream bed. Journal of Hydraulic Engineering 123 (1), 58–64.
Rauen, W.B., Lin, B., Falconer, R.A., 2008a. Transition from wavelets to ripples in a laboratory flume with a diverging channel. International Journal of Sediment Research 23 (1), 1–12.
Rauen, W.B., Lin, B., Falconer, R.A., 2008b. Effect of sediment supply limitation on bed form development under non-uniform flow conditions. Proceedings 3rd International Workshop on Marine and River Dune Dynamics, Leeds, UK, April 2008.
Soulsby, R.L., 1997. Dynamics of Marine Sands – A Manual for Practical Applications. Thomas Telford Publications, London.
Soulsby, R.L., Whitehouse, R.J.S., 2005. Prediction of ripple properties in shelf seas. Mark 1 Predictor, HR Wallingford Report TR 150, Release 1.1.
Yalin, M.S., 1977. Mechanics of Sediment Transport, second ed. Pergamon Press, Guildford.
Yalin, M.S., 1985. On the determination of ripple geometry. Journal of Hydraulic Engineering 111 (8), 1148–1155.